THE JOURNAL OF PHYSICAL CHEMISTRY A

Article

pubs.acs.org/JPCA

Strengthening of the Coordination Shell by Counter Ions in Aqueous Th^{4+} Solutions

Published as part of The Journal of Physical Chemistry virtual special issue "Mark S. Gordon Festschrift".

Raymond Atta-Fynn,*,† Eric J. Bylaska,*,‡ and Wibe A. de Jong*,§

†Department of Physics, The University of Texas at Arlington, Arlington, Texas 76006, United States

‡Environmental Molecular Sciences Laboratory, Pacific Northwest National Laboratory, Richland, Washington 99352, United States

§Computational Research Division, Lawrence Berkeley National Laboratory, Berkeley, California 94720, United States

Supporting Information

ABSTRACT: The presence of counterions in solutions containing highly charged metal cations can trigger processes such as ion-pair formation, hydrogen bond breakages and subsequent re-formation, and ligand exchanges. In this work, it is shown how halide (Cl^-, Br^-) and perchlorate (ClO_4^-) anions affect the strength of the primary solvent coordination shells around Th^{4+} using explicit-solvent and finite-temperature ab initio molecular dynamics modeling methods. The 9-fold solvent geometry was found to be the most stable hydration structure in each aqueous solution. Relative to the dilute aqueous solution, the presence of the counterions did not significantly alter the geometry of the primary hydration shell. However, the free energy analyses indicated that the 10-fold hydrated states were thermodynamically accessible in dilute and bromide aqueous solutions within 1 kcal/mol. Analysis of the results showed that the hydrogen bond lifetimes were longer and solvent exchange energy barriers were larger in solutions with counterions in comparison with the solution with no counterions. This implies that the presence of the counterions induces a strengthening of the Th^{4+} hydration shell.

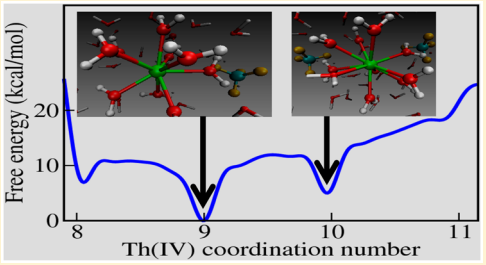

INTRODUCTION

The elucidation of the competing effects of counterions on the hydration shell structure and dynamics of highly charged metal ions in solution, particularly concentrated solutions, is important in its own right: (i) the opposite polarities of the metal cation and the counterions result in Coulomb attractions lead to increased metal ion activity such as ion-pair formation; (ii) counterions can enhance or weaken the hydrogen bond (HB) network between the solvent molecules in the vicinity of the metal ion, and the HB enhancement or weakening subsequently tightens or loosens the solvent geometry around the ion. A direct consequence of (ii) is the prolonged or shortened mean HB lifetimes of the solvent molecules. The latter consequence is equivalent to decreased (prolonged HB lifetime) or increased (shortened HB lifetime) ligand exchange rate. Collectively, all the above-mentioned effects are major factors in the reactivity of the metal ion in solution.

Early work by Choppin[1,2] asserted that as the electrolyte concentration increases, the changes in water coordination are primarily driven by whether or not the counterion was located in the first or second hydration shell. It was rationalized that the coordination numbers of actinide and lanthanide metal cations increase when the counterions are located in the secondary shell and decrease when the counterions are located in the primary shell. However, recent finite-temperature, explicit-solvent ab initio molecular simulations of the Cm^{3+} ion in concentrated solutions containing Cl^- and Br^- and ClO_4^- anions[3] suggested that Choppin's assertion is not necessarily true. Rather, it was observed that changes in the coordination number of Cm^{3+} were dictated by the dynamics of the hydrogen bonds between the solvent−solvent and solvent−counterion pairs. Specifically, the simulations revealed that Cl^- and Br^- tightened the primary hydration shell of Cm^{3+} by polarizing its hydrogen bond network (associated with long mean HB lifetimes), whereas bulky and weakly polarizing ClO_4^- weakened the hydration shell (associated with reduced mean HB lifetimes).

Though the observed counterion effects on the hydrated Cm^{3+} ion provided deep molecular level insights into the solvent shell geometry and hydrogen bond kinetics, it was not obvious whether the effects were generic for metal ions or specific to Cm^{3+}. This motivated us to examine counterion effects in another actinide metal ion in solution. Actinide ions were considered because understanding their interaction with the surrounding environment, particularly their speciation in aqueous environments, is a key aspect of toxic waste remediation. Specifically, a detailed atomistic scale understanding actinide ion speciation in aqueous systems is important as it directly affects the ion's transport, reactivity,

Received: September 29, 2016
Revised: December 1, 2016
Published: December 1, 2016

DOI: 10.1021/acs.jpca.6b09878
J. Phys. Chem. A 2016, 120, 10216−10222

bioavailability, and hence, its potential human and environmental risk.[4]

In this work, we focus on the tetravalent thorium cation (Th^{4+}) in solution. Thorium has attracted a lot of commercial attention because its fuel cycle provides an attractive way to produce long-term nuclear energy with low radiotoxicity waste.[5,6] In this regard, a more thorough understanding of Th-related waste in the environment not only is of fundamental interest but also is potentially relevant to determining its environmental fate and transport. The choice of $Th^{4+}(aq)$ is motivated by lack of a coherent picture in describing its hydration shell from experimental measurements. Furthermore, Th^{4+} is the largest (in terms of ionic radius) stable +4 metal ion in solution,[7] and its relatively large pK_a of approximately 3 (implying that it is fairly resistance to hydrolysis) makes it a suitable model for probing the solvent shell structure of highly charged actinide ions in solution.[8]

Different experimental probes have yielded different results for the hydration shell structures of Th^{4+} in solution. Extended X-ray absorption spectroscopy (EXAFS) experiments have reported primary hydration numbers of 9.8 (0.05 M Th^{4+} in 0.5 M $HClO_4$),[9] 10 ± 1 (0.05 M Th^{4+} in 1.5 M $HClO_4$),[10] 12.7 (0.05 M Th^{4+} in 1.5 M $HClO_4$),[11] and 9 (0.54 M Th^{4+} in 3.16 M $HClO_4$).[8] The average Th−O distance from these EXAFS measurements were 2.44−2.45 Å. Large angle X-ray scattering (LAXS) experiments indicate that the primary hydration numbers of Th^{4+} in $HClO_4$[8,12] and Cl^-[12] solutions are 9 (0.54 M Th^{4+} in 3.16 M $HClO_4$), 8 ± 0.5 (0.99 M Th^{4+} in 5.04 M $HClO_4$), and 10.5 (1.85 M Th^{4+} in 7.40 M Cl), respectively (the average Th−O distances in $HClO_4$ were 2.46[8] and 2.48 Å;[12] in HCl it was 2.51 Å[12]), with the formation of inner sphere complexes in chloride solution. A recent high energy X-ray scattering (HEXs) study on $[Th(OH_2)_{10}]Br_4$ crystal dissolved in water indicated that Th^{4+} was surprisingly homoleptic, that is, no formation of metal−anion pairs, with a primary hydration number of 10.1 and an average Th−O distance of 2.46 Å.[13] The HEXs experiment was based on 278 mg of $Th(H_2O)_{10}Br_4$ in 0.5 g of water at room temperature. This translates to Br and Th concentrations of 2.7 and 0.65 M, respectively. To summarize, there are large uncertainties in the experimental data for the primary hydration number of Th^{4+} in aqueous solution whereas the first shell Th−O distances match quite well.

On the theoretical side, the results are mixed as well. Different coordination numbers in the 8−11 range and Th−O bond distances in the 2.45−2.54 Å range have been reported.[14−18] A bulk of these calculations is based on classical molecular simulations and/or static ab initio geometry optimizations of Th^{4+} hydrates in a parametrized polarizable continuum models. However, it can be quite challenging for parametrized force fields to accurately capture the strong polarization and other chemical interactions of the surrounding water molecules near highly charged metal ions, e.g., a +4 ion. On the contrary, ab initio molecular dynamics (AIMD) significantly accounts for many-body physical and chemical interactions and is therefore the most accurate route to predictive modeling of highly charged ions in aqueous systems. Spezia et al. used AIMD to study the equilibrium hydration shell properties[17] and free energy landscape of the coordination states of Th^{4+} in dilute solution.[18] Their AIMD simulations of Th^{4+} in dilute solution indicated the 9-fold coordinated state is the most stable state. They employed the single sweep method[19] to model the free energy landscape of the Th^{4+} coordination and concluded the 10-fold coordinated state might be thermodynamically accessible with a small energy barrier;[18] the results are compared to our Th^{4+} ion coordination free energy results using metadynamics.[20,21]

COMPUTATIONAL METHODOLOGY

To obtain a parameter-free description of the of Th^{4+} coordination in different aqueous environments, four independent AIMD simulations in the canonical ensemble at 300 K have been carried out for Th^{4+} and ThX_4 (X = ClO_4, Cl, and Br) dissolved in 64 water molecules in a periodic cubic unit cell with the dimension 12.4172 Å (the density of water ≈1 g/cm^3). The concentration of Th^{4+} in each system is 0.86 M; the concentration of counterions in each ThX_4 system is 3.44 M. For the single Th^{4+} ion solution, i.e., when no counteranions are present, the charge at the metal center is neutralized by a uniform background charge of opposite sign: this is the so-called infinite dilution limit (hereafter, we refer to this system as the "dilute solution").[22] The goals of these simulations are to probe the role of counteranions on the geometry of the solvent shell of Th^{4+}, as well as the thermodynamic accessibility of the different coordination states (as characterized by the hydration number) and the dynamical factors which drive the changes in hydration numbers. In probing changes in the ion's first shell coordination number, we are essentially probing ligand exchange between the first shell and the bulk solvents.

The simulations were based on gradient-corrected (PBE) density functional theory[23,24] and the Car−Parrinello molecular dynamics (CPMD) algorithm[25] as implemented in the NWChem computational chemistry code.[26] The free energy landscape characterizing the Th−O coordination in each system was computed using metadynamics.[20,21] Metadynamics accelerates the sampling of the Helmholtz free energy landscape by biasing the dynamics with an external history (i.e., time-dependent) potential that slowly fills the free energy landscape along a few prechosen collective variables (CVs). Here, a single CV was used to describe the energy landscape: the primary coordination number of Th with respect to O as a differentiable function of the atomic coordinates.[27] Additional computational details and parameters are available in the Supporting Information.

A recent theoretical study on liquid water[28] has shown that the BLYP functional[29,30] (with and without Grimme dispersion corrections[31]) yielded liquid water data consistent with experiment. Thus, additional simulations with the BLYP functional[29,30] and BLYP plus Grimme dispersion corrections[31] (Grimme2) were performed to assess the role of the BLYP functional and long-range dispersion effects for each species considered here.

RESULTS AND DISCUSSION

I. PBE Simulations: Metadynamics Free Energies and Hydrogen Bond Lifetimes. The discussions in this section pertain simulations performed with the PBE functional at 300 K. Figure 1 depicts a snapshot of the solvated Th^{4+} ion in the presence of four ClO_4^- anions from the dynamical trajectory; the solvent−solvent and anion-solvent hydrogen bonds are also depicted (see Supporting Information for the hydrogen bonding criteria). The equilibrium properties of each system are reported in Table 1. The first shell Th−O bond distances of 2.48−2.50 Å agree well with prior experimental theoretical data. The equilibrium coordination number is 9, which agrees well

DOI: 10.1021/acs.jpca.6b09878
J. Phys. Chem. A 2016, 120, 10216−10222

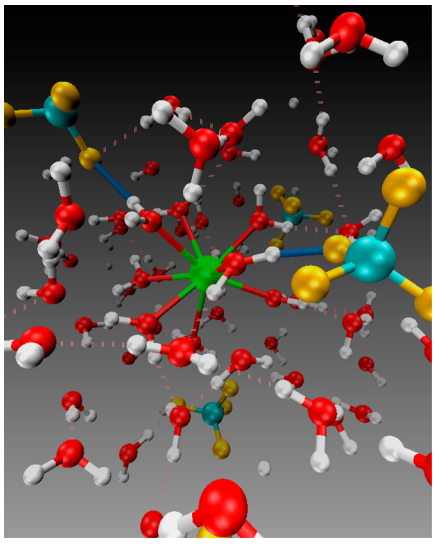

Figure 1. Snapshot of the solvent shell structure of Th^{4+} (green atom) in aqueous solution with ClO_4^- anions (cyan and gold atoms). The broken lines denote the hydrogen bonds between the solvent molecules; solid blue bonds denote hydrogen bonds between ClO_4^- and the solvent molecules.

with the experimental average.[5−10] The geometry of the nine solvent molecules around the ion is a trigonal tricapped prism (see Figure S4 and section 3.2 in the Supporting Information); this structure has been seen in perchlorate solution.[5]

At first glance, the first shell properties in the absence or presence of counterions are nearly the same. However, a closer examination of the radial distribution function indicated that the solvent molecules are slightly less structured around the ion in $Th(ClO_4)_4$ (see Figure S3 and section 3.1 in the Supporting Information). On average, the Cl^- and Br^- counterions are located at the edge of the second shell (cf. r_3 in Table 1), while ClO_4^- remains in the bulk. The presence of the counterions caused small contractions in the second shell Th−O bond distance compared to the dilute solution (cf. r_2 in Table 1). Although the average number hydrogen bonds per solvent molecule reported in Table 2 is nearly the same in each solution, significant differences in the average number of hydrogen bonds formed between the anions and water can be observed. Cl^- and Br^- ions tend to form a well-structured coordination shell (five hydrogen bonds), whereas the ClO_4^- form 2 fewer bonds, implying that ClO_4^- coordinates weakly with water. The reported average number of Br·····H hydrogen bonds n^c_{HB} = 5.2 and corresponding average hydrogen bond distance r^c_{HB} = 2.32 Å (cf. Table 1) are in good agreement with

Table 2. Free Energy Difference $\Delta A_{X\to Y}$ (kcal/mol) between Initial Coordination State *X* and Final State *Y* at 300 K

	$\Delta A_{8\to9}$	$\Delta A_{9\to10}$	$\Delta A_{10\to11}$
Th^{4+}	−5.97	0.87	11.89
$Th(ClO_4)_4$	−6.94	5.00	13.19
$ThCl_4$	−2.84	3.25	11.84
$ThBr_4$	−6.96	1.19	7.27

HEXS experimental values of n^c_{HB} = 6 and r^c_{HB} = 2.30−2.38 Å, respectively.[13]

In Figure 2, the simulated Th^{4+} L_{III} edge k^3 weighted EXAFS spectra of $Th(ClO_4)_4$, $k^3\chi(k)$ is shown, with the experimental

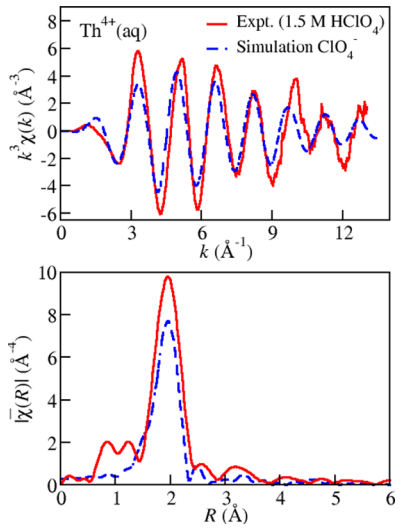

Figure 2. Comparison of the simulated EXAFS spectra (top panel) and corresponding Fourier transform (bottom) with experimental data (ref 10).

data (Th(IV) in 1.5 M $HClO_4$)[10] superimposed for purposes of comparison. The simulated spectrum was obtained using the MD-EXAFS method,[32] which comprises the computation of the spectral average of several snapshots along the molecular dynamical trajectory. The EXAFS spectra of individual snapshots were computed using the ab initio scattering code FEFF.[33] The simulated data match fairly well with the experimental oscillating frequencies and amplitudes up to k = 9 $Å^{-1}$. Beyond this value of k, there are some discrepancies stemming from finite size effects; e.g., the simulation employed a single absorber whereas experimental data are based on multiple absorbers. In the bottom panel, the modulus, $|\overline{\chi}(R)|$, of the Fourier transform of $k^3\chi(k)$ is depicted. Again the

Table 1. Equilibrium Structural Properties of Th^{4+} and Th^{4+} + 4X^- (X= ClO_4, Cl, Br) in Solution at 300 K (Distances in Å, Angles in deg)

	r_1 [a]	N_1 [b]	θ_{tilt} [c]	r_2 [d]	N_2 [e]	n_{HB} [f]	r_3 [g]	n^c_{HB} [h]	r^c_{HB} [i]
Th^{4+}	2.50	9	25	4.70	16	3.4			
$Th(ClO_4)_4$	2.49	9	25	4.63	14	3.5	7.2	3.1	1.90
$ThCl_4$	2.50	9	25	4.64	14	3.6	5.5	5.3	2.20
$ThBr_4$	2.49	9	22	4.65	15	3.6	5.8	5.2	2.32

[a] r_1 is the average first shell Th−O distance in Å. [b] N_1 is the average primary hydration number. [c] θ_{tilt} is the average first shell tilt angle. The computation of θ_{tilt} is in the Supporting Information. [d] r_2 is the average second shell Th−O distance in Å. [e] N_2 is the average second shell hydration number. [f] n_{HB} is the average number of HB per solvent molecule. [g] r_3 is the average Th−anion distance in Å (in the ClO_4^- anions, Cl was used). [h] n^c_{HB} is the average of number HB per anion. [i] r^c_{HB} is the average anion···H hydrogen bond distance in Å (in the ClO_4^- anions, O was used).

DOI: 10.1021/acs.jpca.6b09878
J. Phys. Chem. A 2016, 120, 10216−10222

agreement between theory and experiment is fair. It should be noted that the experimental EXAFS data correspond to a 10 ± 1 coordinated first shell[10] whereas the simulated data corresponding to an 9-fold first shell have a slighly smaller envelope. We note that EXAFS measurements are not very sensitive to small changes in the coordination number.

Figure 3 depicts the converged free energy landscape characterizing different coordination states. To achieve

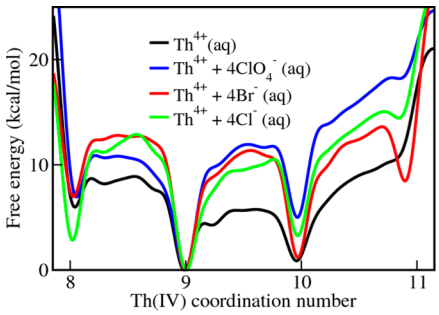

Figure 3. Free energy profiles of each system with the Th^{4+} coordination with respect to O as the collective variable. The lowest energy state is set to zero in each profile.

convergence, the first-principles metadynamics simulations were carried out for a long time scale of 0.1−0.15 ns using a small time step of 0.12 fs (see Figure S6 and section 3.3 in the Supporting Information for proof of convergence).

According to Figure 3, the most stable state in each system is the coordination number 9, which, as expected, is in agreement with the regular molecular dynamics run. The 8 → 9, 9 → 10, and 10 → 11 Helmholtz free energy differences are reported in Table 2. With the free energy differences ΔA, in Table 2, the relative proportions of the 8, 9, 10, and 11 coordination numbers in each system were estimated from $[N + 1] = [N] \exp(-\Delta A_{N\rightarrow N+1}/(k_B T))$, where N = 8, 9, 10, and $[8] + [9] + [10] + [11] = 1$; the results are summarized in Table 3. As

Table 3. Relative Population of 8, 9, 10, and 11 Coordination States in Each System Using the Free Energy Differences in Table 2

	coordination number			
	8	9	10	11
Th^{4+}	0%	81.2%	18.8%	0%
$Th(ClO_4)_4$	0%	100%	0.0%	0%
$ThCl_4$	0.8%	98.8%	0.4%	0%
$ThBr_4$	0%	88.2%	11.8%	0%

expected, coordination number 9 is dominant. The Th^{4+} in dilute solution result of the 9-fold coordination state being more stable is in accordance with recent AIMD simulations by Spezia et al.[18] They found that the other possible stable state is the 10-fold coordination state with the free energy difference between the two states is 3 kcal mol^{-1} and the corresponding barrier is 4 kcal mol^{-1}. The current simulations yielded the free energy difference between the two states is 0.9 kcal mol^{-1} and a barrier of 4.4 kcal mol^{-1}. Hence, our free energy results for Th^{4+} in dilute solution yield results similar to those of Spezia et al.[18]

Regarding the results for ThX_4 (X = ClO_4^-, Cl^-, and Br^-), the 9-fold coordinated state was the most stable and dominant state (cf. Tables 1 and 2). There is, however, a small population of coordination number 8 states present in $Th(ClO_4)_4$ and $ThCl_4$, whereas there is a non-negligible proportion of the coordination number 10 state in dilute solution (19%) and the bromide solution (12%). According to HEX experiments, the coordination number of Th^{4+} in HBr solution is 10, and no Th−Br ion pairs are formed.[13] Although our results indicate that the dominant coordination of Th^{4+} in $ThBr_4$ is not 10, we have shown that the coordination 10 state is within $2k_BT$ from the coordination 9 state in $ThBr_4$ ($\Delta A_{9\rightarrow 10}$ = 1.19 kcal/mol ≈ $2k_BT$) and, therefore, it is thermodynamically accessible. The origin of the difference between the theoretical (9-fold) and experimental (10-fold) observed coordination numbers for $ThBr_4$ is not very clear. The $\Delta A_{9\rightarrow 10}$ is pretty small for $ThBr_4$ (in contrast to the larger values for $ThCl_4$ and $Th(ClO_4)_4$), rendering the possibility of a coordination 10 state likely in an equilibrium simulation. This energy difference is small enough to be affected by finite size and/or density functional effects.

Changes in coordination number essentially constitute a ligand exchange. Ligand exchange is the most fundamental measure of an ion's reactivity in solution. However, if the free energy of the transition state is larger than that of the reactant/product, then the exchange rate will be slower. The activation barrier $\Delta A^{\ddagger}$ between successive coordination states in Figure 3, may be used to characterize associative 9 → 10 exchange (**A**) or dissociative 9 → 8 exchange (**D**). On the basis of only the lowest activation barrier, the **A** mechanism is preferred in dilute solution; in $Th(ClO_4)_4$ **D** is preferred; and in $ThBr_4$ and $ThCl_4$ both **A** and **D** are likely. The **A** mechanism is clearly preferred in dilute solution and $ThBr_4$, and the **D** mechanism is preferred in $Th(ClO_4)_4$. In $ThCl_4$ both the **A** and **D** mechanisms seem likely.

Water exchange reactions between the first shell and the bulk involve the breakage and subsequent re-formation of hydrogen bonds (HBs). The bond breakage and re-formation rates are related to the characteristic bond survival times. In very simple terms, a large exchange reaction barrier implies that the exchanging solvent molecules form HBs that persist for relatively long times, whereas a low exchange reaction barrier implies HBs with relatively short lifetimes. In an attempt to validate the predicted exchange mechanisms, we computed the HB lifetimes from the HB survival time correlation function $S(t)$ (Supporting Information).[34−40] $S(t)$ measures the probability an HB formed between a pair molecules initially at time t = 0 remains continuously alive up to time $t > 0$. Thus, $S(t)$ is the history-dependent[41] probability distribution of the "first HB breaking times" of each initially hydrogen-bonded molecular pair. The characteristic decay time constant, τ, of $S(t)$ is interpreted as the average HB lifetime (Supporting Information). Using the fully equilibrated trajectory for each system, we computed $S(t)$ for the following molecular pairs: (i) first shell solvent molecules (those water molecules coordinated with Th^{4+}) and all other molecules/counterions; (ii) counterions and all solvent molecules.

The top panel of Figure 4 depicts the plots of survival function $S(t)$) for the HBs formed between first shell water molecules and the remaining molecules containing the remaining solvent molecules plus counterions for the PBE functional. The plot in the bottom panel corresponds to the anion−solvent pairs. The associated mean lifetimes τ_1 and τ_2 for the PBE functional are reported in Table 4. The corresponding mean decay times τ_1 reported in Table 4 are smallest in dilute solution. The values of τ_1 for the dilute solution are lower than those for the counterion systems. In

DOI: 10.1021/acs.jpca.6b09878
J. Phys. Chem. A 2016, 120, 10216−10222

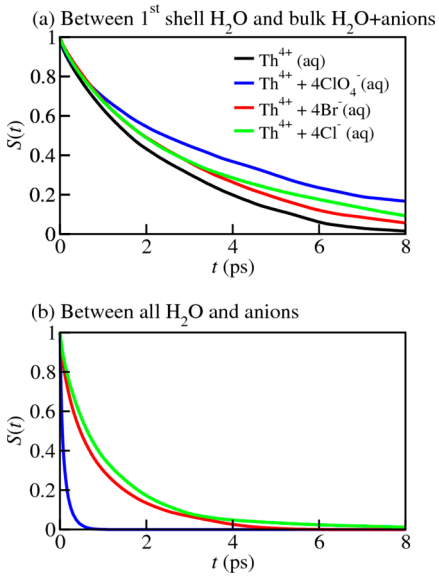

Figure 4. Distribution of lifetimes of hydrogen bonds between (a) first shell water ligands and bulk water-and-anions and (b) anions and water ligands.

Table 4. Mean Hydrogen Bond Lifetimes (ps) for the PBE, BLYP, and BLYP+Grimme2 Computational Models[a]

	PBE		BLYP		BLYP+Grimme2	
	τ_1	τ_2	τ_1	τ_2	τ_1	τ_2
Th^{4+}	2.5		2.4		2.3	
$Th(ClO_4)_4$	4.1	0.1	3.3	0.1	3.6	0.1
$ThCl_4$	3.0	1.1	3.8	1.6	2.3	0.6
$ThBr_4$	3.2	0.9	4.8	0.6	4.7	0.4

[a] τ_1 is the lifetime for the first shell water−bulk water + anion pairs and τ_2 is the lifetime for the first shell water−anion pairs.

accordance with Figure 3, we observe that the 9 → 10 and 9 → 8 energy barriers for the dilute solution are lower than those for the counterion systems. The largest value of τ_1, which corresponds to $Th(ClO_4)_4$, may be interpreted as having the largest exchange reaction barrier. Per Figure 3 this is true in general, though the plot for Br^- solution shows a similar energy barrier. The plots in the lower panel of Figure 4 show that the lifetime of the HBs between the counterions and all solvents. The associated mean lifetimes τ_2 are reported in Table 4. Clearly, τ_2 for Cl^- and Br^- and the solvents are much longer than those of ClO_4^-. The longer HB lifetimes around Cl^- and Br^- are not surprising as experimental measurement of their aqueous solutions have indicated that their mean first shell water residence times are much longer compared with those of neat liquid water, implying that the aqueous solvation shells of these ions are sufficiently rigid.[20] ClO_4^-, however, coordinates weakly in solution.[21]

Interestingly, ClO_4^-, despite its weak coordination in solution, yields the longest mean first hydration shell HB lifetime. It is worth noting that the ClO_4^- ions hardly diffused from their initial local neighborhood during the simulation (see the top panel of Figure S7 in the Supporting Information). To probe the potential dependence of the hydrogen bond lifetimes on the relative position of the ClO_4^- ions, we carried out another simulation where the ions were placed in the second shell. The first shell water hydrogen bond lifetime τ_1 increased to 7.6 ps (compared to τ_1 = 4.1 ps in the original simulation). Furthermore, as was the case in the original simulation, the ClO_4^- ions stayed in the vicinity of the second shell. The lifetime increase is potentially due to formation HBs between the perchlorate oxygen and the primary shell hydrogen. This is opposite to the effect seen in the hydration of the Cm^{3+} ion[3], where the presence of the ClO_4^- ions decreased (weakened) the average HB lifetime (the primary hydration shell). Furthermore, we observed that the presence of ClO_4^- ions increased the equilibrium primary hydration number to 9 relatively to a hydration number of 8 in dilute Cm^{3+} solution.[3] Here no such effect of ClO_4^- on the Th^{4+} hydration number was observed.

II. BYLP and BYLYP+Grimme2 Dispersion Corrections Simulations: Hydrogen Bond Lifetimes. Recent theoretical work on liquid water[28] has shown that the PBE functional[24] leads to overstructured liquid water at 300 K (i.e., the water molecules are less mobile), whereas the BLYP functional[29,30] (with and without Grimme dispersion corrections[31]) yielded liquid water data consistent with experiment. However, it is entirely possible that a density functional that correctly describes liquid water correctly may not necessarily describe the hydration shell geometry and hydrogen bond dynamics of solvated charged ions correctly, due mainly to the strong solvent polarization by the electric field of the ion.

To check the sensitivity of our results to the exchange−correlation functional, we performed additional equilibrium simulations at 300 K for each system using the BLYP functional[29,30] and BLYP functional + Grimme2 corrections[31] and subsequently computed the primary hydration number and hydrogen bond lifetimes.. The primary hydration number of Th^{4+} in these additional simulations was the same as those extracted from equilibrium simulations for the PBE functional (i.e., 9 in each case). The hydrogen bond lifetimes for these simulations are reported in Table 4 together with the PBE results discussed earlier. Though the relative order of the first shell solvent mean HB lifetime τ_1 among the different solutions with counterions does vary for a given functional, these additional simulations show that their τ_1 are consistently longer when compared to that of the dilute solution, validating the key findings of the PBE simulations discussed above. Furthermore, Table 4 also shows that the BLYP simulations yielded values of τ_2 that are not different from the PBE values. In particular, this suggests that the lack of ClO_4^- mobility between shells as discussed earlier is not a functional-dependent issue; it is most likely due to the fact that ClO_4^- is inherently sluggish.

SUMMARY

We have simulated the equilibrium solvent shell properties and the free energy landscape characterized by the coordination states Th^{4+} in dilute, chloride (Cl^-), bromide (Br^-), and perchlorate (ClO_4^-) solutions. More importantly, the free energy differences and activation barriers between neighboring coordination states were computed using ab initio metadynamics. Our work indicates that the most stable state characterized was the 9-fold coordinated state. An important observation in this work was that in the presence of Cl^-, Br^-, and ClO_4^- counterions, water molecules in the first hydration shell had slightly longer hydrogen bond lifetimes compared to the dilute solution.

Free energy analysis at 300 K using the PBE density functional indicated the coordination number of 10 is thermodynamically accessible in dilute solution and $ThBr_4$ solutions. Furthermore, the Cl^-, Br^-, and ClO_4^- anions tend

DOI: 10.1021/acs.jpca.6b09878
J. Phys. Chem. A 2016, 120, 10216−10222

to slow down the first shell ligand exchange rate; this is supported by a qualitative agreement between the exchange barriers and the average hydrogen bond lifetimes between the first shell solvents and remaining solvents and anions. In general, it is found that all three counterions made the first coordination of Th^{4+} more structured by enhancing the first shell HB lifetime. Similar strengthening of the primary shell and slow ligand exchange rate by Cl^- and Br^- counterions have been seen in the hydrated Cm^{3+} ion.[3] This observation was further validated with equilibrium simulations at 300 K using the BLYP functional and BLYP functional with long-range dispersion corrections (Grimme2 corrections).

We believe that counterion effects are very important chemical effects in highly charged and concentrated solutions important in separations chemistry taking place in actinide chemistry processes and in natural geofluid environments that has been for the most part overlooked. Finally, we stress that the methodologies and analyses presented here are useful for characterizing the effects of counterions on the coordination number and associated thermodynamics and solvent hydrogen bond dynamics of hydrated metal ions.

■ ASSOCIATED CONTENT

Supporting Information

The Supporting Information is available free of charge on the ACS Publications website at DOI: 10.1021/acs.jpca.6b09878.

Computational methodologies for ab initio molecular dynamics, ab initio metadynamics, and hydrogen bond dynamics; results on structural properties and metadynamics convergence (PDF)

■ AUTHOR INFORMATION

Corresponding Authors

*R. Atta-Fynn. E-mail: attafynn@uta.edu.
*E. J. Bylaska. E-mail: eric.bylaska@pnnl.gov.
*W. A. de Jong. E-mail: WAdeJong@lbl.gov.

ORCID

Wibe A. de Jong: 0000-0002-7114-8315

Notes

The authors declare no competing financial interest.

■ ACKNOWLEDGMENTS

This research was performed using the Molecular Science Computing Capability in the William R. Wiley Environmental Molecular Science Laboratory (EMSL), a national scientific user facility sponsored by the U.S. Department of Energy's Office of Biological and Environmental Research and located at the Pacific Northwest National Laboratory, operated for the Department of Energy by Battelle. This research also used the resources of the Texas Advanced Computing Center (www.tacc.utexas.edu). Some of the calculations were performed using the Oak Ridge Leadership Computing Facility, which is a DOE Office of Science User Facility supported under Contract DE-AC05-00OR22725. An award of computer time was provided by the Innovative and Novel Computational Impact on Theory and Experiment (INCITE) program. This work was supported by the Heavy Element Chemistry program of the BES Chemical Sciences, Geosciences, and Biosciences, Office of Basic Energy Sciences, U.S. Department of Energy. We thank Drs. Henry Moll, Ingmar Grenthe, and Melissa Denecke for providing the experimental EXAFS data for Th^{4+} in 1.5 M $HClO_4$ solution. We also thank EMSL and the BES Geosciences program for additional support in the development of ab initio dynamics and free energy methods used in this study.

■ REFERENCES

(1) Choppin, G. R.; Jensen, M. P. Actinides in Solution: Complexation and Kinetics. In *The Chemistry of the Actinide and Transactinide Elements*; Moss, L. R., Edelstein, N. M., Fuger, J., Eds.; Springer: Berlin, 2006; p 2524.

(2) Choppin, G. R.; Peterman, D. R. Applications of Lanthanide Luminescence Spectroscopy to Solution Studies of Coordination Chemistry. *Coord. Chem. Rev.* **1998**, *174*, 283.

(3) Atta-Fynn, R.; Bylaska, E. J.; de Jong, W. A. Importance of Counteranions on the Hydration Structure of the Curium Ion. *J. Phys. Chem. Lett.* **2013**, *4*, 2166−2170.

(4) Denecke, M. A. Actinide Speciation Using X-Ray Absorption Fine Structure Spectroscopy. *Coord. Chem. Rev.* **2006**, *250*, 730.

(5) Greenwood, N. N.; Earnshaw, A. *Chemistry of the Elements*, Second ed.; Pergamon Press Ltd.: Elmsford, NY, 1997.

(6) *Thorium fuel cycle — Potential benefits and challenges*; International Atomic Energy Agency: Vienna, 2005.

(7) Shannon, R. Revised Effective Ionic Radii and Systematic Studies of Interatomic Distances in Halides and Chalcogenides. *Acta Crystallogr., Sect. A: Cryst. Phys., Diffr., Theor. Gen. Crystallogr.* **1976**, *32*, 751−767.

(8) Torapava, N.; Persson, I.; Eriksson, L.; Lundberg, D. Hydration and Hydrolysis of Thorium(Iv) in Aqueous Solution and the Structures of Two Crystalline Thorium(Iv) Hydrates. *Inorg. Chem.* **2009**, *48*, 11712.

(9) Hennig, C.; Schmeide, K.; Brendler, V.; Moll, H.; Tsushima, S.; Scheinost, A. C. Exafs Investigation of U(Vi), U(Iv), and Th(Iv) Sulfato Complexes in Aqueous Solution. *Inorg. Chem.* **2007**, *46*, 5882.

(10) Moll, H.; Denecke, M. A.; Jalilehvand, F.; Sandström, M.; Grenthe, I. Structure of the Aqua Ions and Fluoride Complexes of Uranium(Iv) and Thorium(Iv) in Aqueous Solution an Exafs Study. *Inorg. Chem.* **1999**, *38*, 1795.

(11) Rothe, J.; Denecke, M. A.; Neck, V.; Müller, R.; Kim, J. I. Xafs Investigation of the Structure of Aqueous Thorium(Iv) Species, Colloids, and Solid Thorium(Iv) Oxide/Hydroxide. *Inorg. Chem.* **2002**, *41*, 249−258.

(12) Johansson, G.; Magini, M.; Ohtaki, H. Coordination around Thorium(Iv) in Aqueous Perchlorate, Chloride and Nitrate Solutions. *J. Solution Chem.* **1991**, *20*, 775.

(13) Wilson, R. E.; Skanthakumar, S.; Burns, P. C.; Soderholm, L. Structure of the Homoleptic Thorium(Iv) Aqua Ion $[Th(H_2o)_{10}]Br_4$. *Angew. Chem., Int. Ed.* **2007**, *46*, 8043.

(14) Yang, T.; Tsushima, S.; Suzuki, A. Quantum Mechanical and Molecular Dynamical Simulations on Thorium(Iv) Hydrates in Aqueous Solution. *J. Phys. Chem. A* **2001**, *105*, 10439.

(15) Yang, T.; Tsushima, S.; Suzuki, A. Chloride Concentration and Temperature Effects on the Hydration of Th(Iv) Ion: A Molecular Dynamics Simulation. *Chem. Phys. Lett.* **2002**, *360*, 534.

(16) Réal, F.; Trumm, M.; Vallet, V. r.; Schimmelpfennig, B.; Masella, M.; Flament, J.-P. Quantum Chemical and Molecular Dynamics Study of the Coordination of Th(Iv) in Aqueous Solvent. *J. Phys. Chem. B* **2010**, *114*, 15913.

(17) Spezia, R.; Beuchat, C.; Vuilleumier, R.; D'Angelo, P.; Gagliardi, L. Unravelling the Hydration Structure of Thx_4 (X = Br, Cl) Water Solutions by Molecular Dynamics Simulations and X-Ray Absorption Spectroscopy. *J. Phys. Chem. B* **2012**, *116*, 6465.

(18) Spezia, R.; Jeanvoine, Y.; Beuchat, C.; Gagliardi, L.; Vuilleumier, R. Hydration Properties of Cm(Iii) and Th(Iv) Combining Free Energy Profiles with Electronic Structure Analysis. *Phys. Chem. Chem. Phys.* **2014**, *16*, 5824−5832.

(19) Maragliano, L.; Vanden-Eijnden, E. Single-Sweep Methods for Free Energy Calculations. *J. Chem. Phys.* **2008**, *128*, 184110.

DOI: 10.1021/acs.jpca.6b09878
J. Phys. Chem. A 2016, 120, 10216−10222

(20) Laio, A.; Parrinello, M. Escaping Free-Energy Minima. *Proc. Natl. Acad. Sci. U. S. A.* **2002**, *99*, 12562.
(21) Laio, A.; Gervasio, F. L. Metadynamics: A Method to Simulate Rare Events and Reconstruct the Free Energy in Biophysics, Chemistry and Material Science. *Rep. Prog. Phys.* **2008**, *71*, 126601.
(22) Gaiduk, A. P.; Zhang, C.; Gygi, F.; Galli, G. Structural and Electronic Properties of Aqueous Nacl Solutions from Ab Initio Molecular Dynamics Simulations with Hybrid Density Functionals. *Chem. Phys. Lett.* **2014**, *604*, 89−96.
(23) Kohn, W.; Sham, L. J. Self-Consistent Equations Including Exchange and Correlation Effects. *Phys. Rev.* **1965**, *140*, A1133.
(24) Perdew, J. P.; Burke, K.; Ernzerhof, M. Generalized Gradient Approximation Made Simple. *Phys. Rev. Lett.* **1996**, *77*, 3865.
(25) Car, R.; Parrinello, M. Unified Approach for Molecular Dynamics and Density-Functional Theory. *Phys. Rev. Lett.* **1985**, *55*, 2471.
(26) Valiev, M.; et al. Nwchem: A Comprehensive and Scalable Open-Source Solution for Large Scale Molecular Simulations. *Comput. Phys. Commun.* **2010**, *181*, 1477.
(27) Sprik, M. Coordination Numbers as Reaction Coordinates in Constrained Molecular Dynamics. *Faraday Discuss.* **1998**, *110*, 437.
(28) Lin, I. C.; Seitsonen, A. P.; Tavernelli, I.; Rothlisberger, U. Structure and Dynamics of Liquid Water from Ab Initio Molecular Dynamics—Comparison of Blyp, Pbe, and Revpbe Density Functionals with and without Van Der Waals Corrections. *J. Chem. Theory Comput.* **2012**, *8*, 3902−3910.
(29) Becke, A. D. Density-Functional Exchange-Energy Approximation with Correct Asymptotic Behavior. *Phys. Rev. A: At., Mol., Opt. Phys.* **1988**, *38*, 3098−3100.
(30) Lee, C.; Yang, W.; Parr, R. G. Development of the Colle-Salvetti Correlation-Energy Formula into a Functional of the Electron Density. *Phys. Rev. B: Condens. Matter Mater. Phys.* **1988**, *37*, 785−789.
(31) Grimme, S.; Antony, J.; Ehrlich, S.; Krieg, H. A Consistent and Accurate Ab Initio Parametrization of Density Functional Dispersion Correction (Dft-D) for the 94 Elements H-Pu. *J. Chem. Phys.* **2010**, *132*, 154104.
(32) Dang, L. X.; Schenter, G. K.; Glezakou, V. A.; Fulton, J. L. Molecular Simulation Analysis and X-Ray Absorption Measurement of Ca^{2+}, K^{+} and Cl^{-} Ions in Solution. *J. Phys. Chem. B* **2006**, *110*, 23644.
(33) Rehr, J. J.; Kas, J. J.; Vila, F. D.; Prange, M. P.; Jorissen, K. Parameter-Free Calculations of X-Ray Spectra with Feff9. *Phys. Chem. Chem. Phys.* **2010**, *12*, 5503−5513.
(34) Luzar, A.; Chandler, D. Structure and Hydrogen Bond Dynamics of Water−Dimethyl Sulfoxide Mixtures by Computer Simulations. *J. Chem. Phys.* **1993**, *98*, 8160.
(35) Luzar, A.; Chandler, D. Effect of Environment on Hydrogen Bond Dynamicsin Liquid Water. *Phys. Rev. Lett.* **1996**, *76*, 928.
(36) Luzar, A. Resolving the Hydrogen Bond Dynamics Conundrum. *J. Chem. Phys.* **2000**, *113*, 10663.
(37) Starr, F. W.; Nielsen, J. K.; Stanley, H. E. Fast and Slow Dynamics of Hydrogen Bonds in Liquid Water. *Phys. Rev. Lett.* **1999**, *82*, 2294−2297.
(38) Chandra, A. Effects of Ion Atmosphere on Hydrogen-Bond Dynamics in Aqueous Electrolyte Solutions. *Phys. Rev. Lett.* **2000**, *85*, 768.
(39) Rapaport, D. C. Hydrogen Bonds in Water. *Mol. Phys.* **1983**, *50*, 1151.
(40) Stillinger, F. H. Theory and Molecular Models for Water. *Adv. Chem. Phys.* **1975**, *31*, 1.
(41) "History-dependent" here simply means that the continuous presence of the hydrogen bond is required.

DOI: 10.1021/acs.jpca.6b09878
J. Phys. Chem. A 2016, 120, 10216−10222